HHS Public Access

Author manuscript

Ann Rheum Dis. Author manuscript; available in PMC 2016 June 01.

Published in final edited form as:

Ann Rheum Dis. 2015 December ; 74(12): 2236–2243. doi:10.1136/annrheumdis-2014-205799.

B-cell depletion attenuates serological biomarkers of fibrosis and myofibroblast activation in IgG4-related disease

Emanuel Della-Torre[1,2], **Eoin Feeney**[3], **Vikram Deshpande**[4], **Hamid Mattoo**[1], **Vinay Mahajan**[1], **Maria Kulikova**[1], **Zachary S Wallace**[5], **Mollie Carruthers**[5], **Raymond T Chung**[3], **Shiv Pillai**[1], and **John H Stone**[5]

[1]Massachusetts General Hospital Cancer Center, Boston, Massachusetts, USA

[2]Unit of Medicine and Clinical Immunology, IRCCS-San Raffaele Scientific Institute, Università Vita-Salute San Raffaele, Milan, Italy

[3]Liver Center and Division of Gastroenterology, Massachusetts General Hospital, Boston, Massachusetts, USA

[4]Department of Pathology, Massachusetts General Hospital, Boston, Massachusetts, USA

[5]Division of Rheumatology, Allergy, and Immunology, Massachusetts General Hospital, Boston, Massachusetts, USA

Abstract

Objectives—Fibrosis is a predominant feature of IgG4-related disease (IgG4-RD). B-cell depletion induces a prompt clinical and immunological response in patients with IgG4-RD, but the effects of this intervention on fibrosis in IgG4-RD are unknown. We used the enhanced liver fibrosis (ELF) score to address the impact of rituximab on fibroblast activation. The ELF score is an algorithm based on serum concentrations of procollagen-III aminoterminal propeptide, tissue inhibitor of matrix metalloproteinase-1 and hyaluronic acid.

Methods—Ten patients with active, untreated IgG4-RD were enrolled. ELF scores were measured and correlated with the IgG4-RD Responder Index, serum IgG4, circulating plasmablasts and imaging studies. Through immunohistochemical stains for CD3, CD20, IgG4 and α-smooth muscle actin, we assessed the extent of the lymphoplasmacytic infiltration and the degree of fibroblast activation in one patient with tissue biopsies before and after rituximab.

Results—The ELF score was increased in patients with IgG4-RD compared with healthy controls (8.3±1.4 vs 6.2±0.9; p=0.002) and correlated with the number of organs involved (R^2=0.41; p=0.04). Rituximab induced significant reductions in the ELF score, the number of circulating plasmablasts and the IgG4-RD Responder Index (p<0.05 for all three parameters).

Correspondence to Dr John H Stone, Rheumatology Clinic/Yawkey 2, Massachusetts General, Hospital, 55 Fruit Street, Boston, MA 02114, USA; jhstone@mgh.harvard.edu.

Contributors All have read and approved the final version of the manuscript.

Patient consent Obtained.

Ethics approval This study was approved by the Institutional Review Board of Partners.

Data sharing statement The investigators will consider sharing any original but unpublished data from this study upon the receipt of a written request.

Rituximab reduced both the lymphoplasmacytic infiltrate and myofibroblast activation. IgG4-RD relapse coincided with recurrent increases in the ELF score, indicating reactivation of collagen deposition.

Conclusions—The ELF score may be a clinically useful indicator of active fibrosis and the extent of disease in IgG4-RD. B-cell depletion has the potential to halt continued collagen deposition by attenuating the secretory phenotype of myofibroblasts in IgG4-RD lesions.

INTRODUCTION

IgG4-related disease (IgG4-RD) is a fibroinflammatory condition generally characterised by tumefactive lesions and often by elevated serum IgG4 concentrations.[1] IgG4-RD was originally defined in the context of type 1 autoimmune pancreatitis, but subsequently has been described in nearly every organ system.[1–9] Typical pathological findings include dense tissue fibrosis with a storiform pattern, a diffuse lymphoplasmacytic infiltrate with an abundance of IgG4-positive plasma cells, mild to moderate eosinophilia and obliterative phlebitis. The fibrosis, a major feature of IgG4-RD, arises from collagenous and non-collagenous extracellular matrix components produced by the large number of myofibroblasts present within tissue lesions. These cells are often overlooked amid the lymphoplasmacytic infiltrate.[2]

Our knowledge of the pathophysiology of IgG4-RD is evolving rapidly.[10] One major hypothesis contends that T lymphocytes produce profibrotic cytokines, such as interleukin (IL)-10, transforming growth factor (TGF)-β, IL-4 and IL-13, which drive the observed B-cell commitment to IgG4-secreting plasma cells as well as the deposition of extracellular matrix by activated fibroblasts.[10] B-cell depletion therapy induces a swift clinical improvement and a prompt serum IgG4 reduction in patients with IgG4-RD, suggesting that response to rituximab is attributable at least in part to the inability to replete stores of short-lived plasma cells.[1112]

Clinical improvement correlates also with a substantial diminution of circulating plasmablasts, the precursors of plasma cells, now known to be markedly increased in active IgG4-RD.[13–15] Clinical relapses of IgG4-RD following rituximab-mediated B-cell depletion correspond to the re-emergence of ‘clonally divergent’ plasmablasts.[14] The tight correlation between circulating plasmablast counts, IgG4-RD disease activity and the response to rituximab-mediated B-cell depletion suggests an important contribution of the B-cell lineage to the pathophysiology of this fibrotic disorder. However, the direct effects of rituximab on fibroblasts and collagen deposition in IgG4-RD have never been investigated.

In the present study, we used the enhanced liver fibrosis (ELF) score in order to address the impact of immunosuppressive therapy on fibrosis in IgG4-RD. The ELF score is a clinically validated surrogate marker of the severity of tissue fibrosis and a predictor of clinical outcomes in the setting of chronic fibrotic liver diseases and systemic sclerosis.[1617] The ELF score assesses the degree of extracellular matrix deposition by measuring the serum concentrations of three analytes involved in both fibrogenesis and remodelling of the extracellular matrix. These analytes are: (1) hyaluronic acid (HA); (2) amino-terminal propeptide of procollagen type III (PIIINP) and (3) tissue inhibitor of matrix

metalloproteinase-1 (TIMP-1). We also examined the degree of fibroblast activation before and after rituximab administration, through immunohistochemical analysis of skin biopsies from a patient with IgG4-RD involvement of the skin.

PATIENTS AND METHODS

Patients and samples

The study was approved by the Institutional Review Board and all subjects provided informed, written consent for the analyses performed. From the database of the Massachusetts General Hospital Center for IgG4-Related Disease, we identified ten patients with active, biopsy-proven IgG4-RD. All patients met the following inclusion criteria: absence of hepatic involvement by IgG4-RD, negative serologies for hepatitis B or C infections, no history of alcohol abuse and normal serum values of hepatic aminotransferases. Additionally, patients were not on glucocorticoid treatment at the time of enrolment. The IgG4-RD Responder Index (RI) was used to characterise patients' clinical status as either active disease (RI≥3) or in remission (RI<3).[18] Eight healthy individuals (mean age 50 years, range 36–56 years) were chosen as controls. Patients were treated with 1000 mg of rituximab in two doses separated by 15 days and did not receive glucocorticoid therapy during follow-up. Peripheral blood was collected at the time of clinical assessment.

Plasma was separated and stored at −20°C. Post-therapy samples were collected on an average of 4 months (range 3–5 months) after treatment. Patients were followed for a mean of 17 months (range 9–24 months) after receiving their first rituximab infusion. All imaging studies were performed within 20 days of the collection of blood samples.

ELF score

The ELF score consists of a single value derived from an algorithm that combines quantitative plasma measurements of HA, PIIINP and TIMP-1.[19,20] Plasma concentrations of these three analytes were measured using quantitative ELISA for HA and TIMP-1 (R&D Systems, Minneapolis, USA) and PIIINP (USCN Life, Wuhan, China). The assays were calibrated using standards provided by the manufacturer. The ELF score was derived from these parameters using the following formula, which is employed by the commercially available ELF test for clinical use (Advia Centaur CP platform)

$$\text{ELF score} = 2.494 + 0.846 \ln(C_{HA}) + 0.735 \ln(C_{PIIINP}) + 0.391 \ln(C_{TIMP-1}).$$

Flow cytometric analysis

Mononuclear cells were isolated from peripheral blood by Ficoll–Paque Plus (GE Healthcare) density-gradient centrifugation following the manufacturer's protocol and resuspended in fetal bovine serum containing 10% dimethyl sulfoxide for cryopreservation in liquid nitrogen for subsequent flow cytometric analysis. Fluorescent labelling for flow cytometry was performed by incubating cells in staining buffer (Biolegend) containing optimised concentrations of the following fluorochrome-conjugated monoclonal antibodies: antihuman CD19-Pacific Blue (clone HIB19, Biolegend), antihuman CD27-APC (clone O323, Biolegend) and antihuman CD38-FITC (clone HIT2, Biolegend). Flow cytometry was performed on a BD LSR II (BD Biosciences) and the fcs files were analysed using

FlowJo software (V.9.6.3, Treestar). The plasmablast population was defined as $CD19^+CD27^+CD38^+$ cells.[13]

Skin biopsies and immunohistochemical analysis

Skin biopsy specimens were obtained from a patient with cutaneous IgG4-RD involvement at the same site on the left cheek, before and 2 weeks after treatment with rituximab. Sections from formalin-fixed, paraffin-embedded tissues were stained for CD20 (Leica; dilution 1:100), CD3 (Leica; ready to use) and α-smooth muscle actin (α-SMA) (Leica; ready to use), in order to identify B cells, T cells and myofibroblasts, respectively. Sections were also stained for IgG4 (Cell Marque; dilution 1:25).

Morphometric analysis

Slides from skin biopsies were scanned using the Aperio ScanScope CS system (Aperio Technologies, Vista, California, USA) and quantitative analyses were performed with the Aperio ImageScope program. The Positive Pixel Count Algorithm was used to calculate the number of brown pixels per square micrometer on the α-SMA preparation. Vascular structures and smooth muscle cells, normal components of the skin, were excluded from the analysis. Fibroblasts, $IgG4^+$ plasma cells and $CD3^+$ T cells were counted manually on both the prerituximab and postrituximab treatment tissues.

Statistical analysis

Statistical analysis was performed using GraphPad Prism software V.6.0. Unpaired and paired t test, when indicated, were used to perform comparisons between two groups. Parametric correlations were calculated using Pearson's correlation test. A p value <0.05 was considered significant. Continuous variables are expressed as mean±SD, unless otherwise specified.

RESULTS

Clinical, serological and immunological characteristics of the patient cohort

Patient characteristics are summarised in the online supplementary table S1. The mean age of the 10 patients with IgG4-RD was 67 years (range 42–80 years), with a male to female ratio of 4:1. The mean age of the healthy controls was 50 years (range 36–56 years), with a male to female ratio of 7:1. At the time of diagnosis, six patients presented with multiorgan disease and four with singleorgan disease involvement, either orbital pseudotumour or retroperitoneal fibrosis. The most commonly involved organs were the parotid glands, the pancreas and retroperitoneum (five cases). Other sites of involvement included the submandibular glands, kidneys, lungs and orbits (four cases each); the lacrimal glands (three cases); the aorta (two cases) and the lymph nodes, pericardium and skin (one case each).

All patients had active disease at the time their blood samples were collected, as demonstrated by the mean IgG4-RD RI of 13.1 (range 4–37). Additionally, none of the patients were on any immunosuppressive therapy when their samples were drawn. The erythrocyte sedimentation rate (ESR) was increased in eight patients (mean 64 mm/h; range 26–92; normal <20 mm/h). The C-reactive protein (CRP) was elevated in five patients

(mean 60 mg/L; range 19–117; normal <8 mg/L). The serum IgG4 concentrations were elevated in eight patients, with a mean value of 1579 mg/dL (range 208–4780 mg/dL; normal <121 mg/dL). Total circulating plasmablasts were increased in all 10 patients with a mean value of 17 600 cells/mL (range 2160–66 237; normal <900 cells/mL).

The ELF score is increased in IgG4-RD and correlates with the number of organs involved

HA, TIMP-1 and PIIINP concentrations were elevated significantly among the patients with IgG4-RD compared with healthy controls (see online supplementary figure S1). The mean plasma level of HA, TIMP-1 and PIIINP in these patients was 32.0 ±18.6 (vs 8.9±3.1 for the controls), 110.2±37.7 (vs 52.5 ±19.9) and 8.3±6.4 (vs 2.1±1.3), respectively ($p<0.01$ for all comparisons). The corresponding mean ELF scores were 8.3±1.4 in the patients with IgG4-RD, compared with 6.2±0.9 in the controls ($p=0.002$) (figure 1A). The ELF scores for each patient are reported in the online supplementary table S1. The values of each ELF score component for each patient before rituximab are reported in the online supplementary table S2. Of note, the two patients with IgG4-RD limited to the orbit had ELF scores of 5.8 and 5.6, comparable with the ELF scores of the healthy controls. Linear regression analysis was performed in order to exclude the possible influence of variables other than collagen metabolism on the fibrosis score. The ELF score did not correlate with CRP ($R^2=0.13$; $p=0.29$), ser um IgG4 concentration ($R^2=0.08$; $p=0.41$), IgG4-RD RI ($R^2=0.12$; $p=0.31$) or circulating plasmablast levels ($R^2=0.02$; $p=0.67$). The ELF score did correlate positively with both the numbers of organs involved ($R^2=0.41$; $p=0.04$) (figure 1B) and the ESR ($R^2=0.39$; $p=0.06$) (data not shown), although the latter comparison did not achieve statistical significance. These results indicate that the ELF score is a useful assessment of active fibrosis in IgG4-RD and is directly proportional to the number of organs involved.

The ELF score decreases following rituximab treatment

In order to assess the effects of B-cell depletion therapy on the fibrotic process, samples were collected and analysed on average 4 months (range 3–5 months) after the first infusion of rituximab. Treatment with rituximab induced a significant reduction in the ELF score ($p=0.004$) (figure 2A). Among the eight patients with IgG4-RD with elevated ELF scores at baseline, the scores declined in all and were indistinguishable from healthy controls in four. The time course of each ELF score component for each patient is reported in the online supplementary table S2. The two patients with disease localised to orbit—who had the lowest ELF scores among the IgG4-RD subjects studied—also declines in their ELF scores after treatment. The mean ELF score for all patients after treatment with rituximab decreased by ~25% to 6.3±2.0, comparable with that of the healthy controls.

Paired t test analyses of the IgG4-RD RI and the circulating plasmablast counts before and after rituximab therapy revealed significant reductions following treatment ($p=0.004$ and $p=0.04$, respectively) (figure 2A). During the period between baseline measurement and the follow-up assessment, three of the patients with IgG4-RD achieved IgG4-RD RI values ≤3 and seven still had IgG4-RD RI values ≥3 (the mean IgG4-RD RI score declined from 13.1 at baseline to 4.4 at follow-up; $p=0.004$). Similarly, the concentrations of circulating plasmablasts normalised in five patients (of whom two achieved IgG4-RD RI scores ≤3) and remained above normal in five patients (of whom one achieved IgG4-RD RI scores ≤3).

Treatment with rituximab typically reduced the dimensions of the inflammatory masses on imaging studies and was accompanied by decreased 18-fluorodeoxyglucose uptake on positron emission tomography scan (figure 2B). Complete disappearance of the tumefactive lesion rarely occurred, however, and residual disease tissue persisted in the majority of patients. In one patient (#355), despite complete depletion of the circulating plasmablasts, a marked clinical response and normalisation of the ELF score, the radiological appearance of the IgG4-RD lesion in the retroperitoneum remained grossly unchanged (figure 2B). The reduction in ELF scores following rituximab therapy is consistent with the concept that B-cell depletion leads to a reduction in the degree of myofibroblast activation in IgG4-RD. However, clinical remission as well as normalisation of the ELF score may not correspond to the complete resolution of the fibrotic lesions.

Fibroblast activation decreases after treatment with rituximab

We assessed the fibroblast activation status in skin biopsies obtained from the same site in a patient with indurated papulonodular lesions resulting from cutaneous IgG4-RD involvement using a histological approach before and after treatment with rituximab. In the treatment-naive tissue, the myofibroblasts exhibited voluminous cytoplasm with a strong cytoplasmic reactivity for α-SMA, suggesting that they were in an activated state (figures 3 and 4A, B). Following B-cell depletion, marked dimunition in both cytoplasmic volume and α-SMA filaments were noted, together with a reduction of the total number of myofibroblasts (figures 3 and 4C, D). In particular, the number of moderately to strongly positive brown pixels per square micrometer in the regions containing predominantly dermal fibroblasts was 0.65 before therapy and 0.23 after therapy, amounting to a reduction in overall signal intensity of 66% (figure 3). This is indicative of a reduction in the number of SMA fibres in the myofibroblasts after rituximab-induced remission. Additionally, α-SMA$^+$ dermal myofibroblast density showed a reduction from 1239 cells/mm^2 before treatment to 1030 cells/mm^2 after rituximab therapy (see online supplementary figure S2).

Rituximab administration also led to a significant reduction in both IgG4$^+$ plasma cells and CD3$^+$ T cells within the lymphoplasmocytic infiltrate (figure 5). Histological improvement corresponded with clinical resolution of the skin lesions (figure 5). In sum, these findings indicate that the reduction in the B-cell and T-cell infiltrate affects the functional phenotype of myofibroblasts by decreasing the degree of myofibroblast activation in affected tissues. The effect of B-cell depletion therapy on the overall number of myofibroblasts was less significant in this case.

IgG4-RD relapse is associated with an increase in the ELF score

IgG4-RD relapsed in Patients 361 and 365, 11 and 13 months after the first course of rituximab, respectively, and was associated with re-emergence of circulating plasmablasts and a worsening IgG4-RD RI as previously reported[13]; in both patients, clinical relapse was also associated with a rise in ELF scores (figure 6A). Corresponding imaging studies revealed the progression of the known lesions in the periaortic tissue, parotid and submandibular glands in Patient #361, and the appearance of new lung nodules in Patient #365. Of note, the findings of retroperitoneal fibrosis in Patient #365 remained stable on repeat cross-sectional imaging (figure 6B). These observations support the notion that

clinical relapse in IgG4-RD following rituximab therapy coincides with reactivation of myofibroblasts and collagen deposition in the sites of active disease.

DISCUSSION

New aspects of the full potential impact of B-cell depletion continue to be recognised more than 15 years after rituximab was approved for the treatment of lymphoma in 1997. Recent results in patients with systemic sclerosis and interstitial lung disease suggest that B-cell depletion has a role in the treatment of systemic fibrotic conditions, a concept that extends far beyond the overly simplistic view about B cells as just precursors of antibody-producing plasma cells.[21–23] In IgG4-RD, a newly described fibroinflammatory disease, B-cell depletion induces a prompt clinical response with a drastic reduction in a population of circulating plasmablasts that are oligoclonally expanded during active disease.[1314] These data support a possible pathogenic role of B lymphocytes, but the precise mechanism(s) through which rituximab affects fibrosis in IgG4-RD remains elusive. In order to address this issue, we adopted the ELF score as a surrogate marker of the fibrotic process and evaluated myofibroblast activity in the tissue before and after treatment using circulating biomarkers of fibrosis. Our data demonstrate that B-cell depletion has the potential to halt collagen production by affecting the secretory phenotype of myofibroblasts in IgG4-RD lesions.

Rituximab might impair several pathways through which B lymphocytes (activated or memory B lymphocytes as well as plasma cells) may potentially sustain extracellular matrix deposition, including (1) a contact-dependent crosstalk with fibroblasts[2425]; (2) the production of profibrotic cytokines, such as IL-6 and TGFβ[26] and (3) the secretion of autoantibodies that directly stimulate fibroblasts or inhibit metalloproteinase activity.[27] In theory, cytokines that mediate fibroblast activation might also be released by the expanded population of plasmablasts that we have observed in the blood and tissues of patients with active IgG4-RD,[1314] but the secretory potential of these plasmablasts has not yet been comprehensively analysed. Additionally, apart from depleting $CD20^+$ B cells and CD20− plasmablasts that are derived from the former, rituximab might interfere with B-cell/T-cell crosstalk through the elimination of a major B-cell type required for continuous antigen presentation to T cells and for the maintenance of T-cell activation.[28] In this sense, it is tempting to speculate that B-cell depletion ultimately abrogates the secretion of profibrotic cytokines (eg, IL-4, IL-13, IL-10 and others) by T-cell populations, as well. These hypotheses are not mutually exclusive and may, in fact, all contribute to the reduced systemic collagen deposition observed in our study after B-cell depletion. On the other hand, it is unlikely that rituximab directly targets myofibroblasts, which do not express CD20 on their surface.

All in all, rituximab primarily affects fibrosis in IgG4-RD by causing activated myofibroblasts to revert to a quiescent state. Indeed, in physiological conditions, tissue-resident fibroblasts are found in a resting state, although they are metabolically active and biomechanically support organ structure and function. In the presence of pro-fibrotic stimuli, such as those induced during tissue repair, regeneration or inflammation, myofibroblasts become activated and synthetically active, expressing α-SMA and secreting copious

amounts of extracellular matrix.[29–32] Upon cessation of these pro-fibrotic stimuli, some myofibroblasts undergo apoptosis. A substantial proportion of myofibroblasts escape this fate, however; these survive to downregulate fibrogenic genes, upregulate antiapoptotic pathways and acquire a quiescent phenotype, similar to that observed in the myofibroblasts following treatment in this study.[3334] Analogous mechanisms secondary to B-cell depletion might affect the dynamics of collagen deposition observed in IgG4-RD, as well. We note that the effects reported in our study were linked specifically to B-cell depletion, because our patients did not receive longitudinal treatment with glucocorticoids or other immunosuppressive therapies. Indeed, glucocorticoids are known to inhibit fibroblast growth and collagen production.[35]

The clinical and histological data presented (figures 3–5) support the idea that the swift shrinkage of the skin lesions observed in our patient following B-cell depletion is attributable to a rapid reduction in the lymphoplasmocytic infiltrate as well as fibroblast activity. By extension, mass-forming IgG4-RD lesions are more likely to shrink in the presence of a lymphoplasmocytic infiltrate and activated myofibroblasts (‘active fibrosis’) rather than in the presence of tightly organised collagen bundles in which both inflammatory cells and myofibroblasts are scarce (‘acellular end-stage fibrosis’ or ‘fibrotic scar’). These findings underscore the value of early treatment, designed to prevent end-stage fibrosis that is less likely to respond to currently available therapies.

The two disease relapses in this study corresponded to the re-emergence of circulating plasmablasts and to renewed elevations of the ELF score, implying that IgG4-RD flares are characterised by both immune activation and extracellular matrix deposition. This is precisely what is observed under the microscope in the histopathology of this condition: an intense lymphoplasmacytic infiltrate accompanied by fibrosis, even in the earliest stages of disease. Indeed, quiescent fibroblasts are known to retain the ability to reactivate rapidly into myofibroblasts if new or recurrent fibrogenic stimuli are encountered.[34] This also suggests the potential clinical utility of the ELF score in monitoring IgG4-RD activity, although it has to be validated in a larger number of patients. Further studies are also warranted in order to address the possibility of integrating this and other serum biomarkers into a revised IgG4-RI.

In conclusion, we show that extracellular matrix deposition is increased in active IgG4-RD and that the associated fibrosis can be halted by B-cell depletion therapy. In particular, disappearance of B and T lymphocytes from the tissue correlates with the reduction in myofibroblast activation, suggesting a pathogenic cross-talk between these cells. The identification of the major cell type initiating the fibrotic cascade in IgG4-RD could provide additional pathogenic clues and alternative therapeutic targets for human fibrotic disorders in general.

Supplementary Material

Refer to Web version on PubMed Central for supplementary material.

Acknowledgments

Funding This work was funded in part by grants AI 064930 and AI 076505 from the National Institutes of Health and by the Autoimmunity Center of Excellence in IgG4-RD, funded by the National Institute of Allergy and Infectious Diseases.

Competing interests JHS and SP have consulted for Genentech on IgG4-related disease.

REFERENCES

1. Stone JH, Zen Y, Deshpande V. IgG4-related disease. N Engl J Med. 2012; 366:539–551. [PubMed: 22316447]
2. Deshpande V, Zen Y, Chan JK, et al. Consensus statement on the pathology of IgG4-related disease. Mod Pathol. 2012; 25:1181–1192. [PubMed: 22596100]
3. Stone JH, Khosroshahi A, Deshpande V, et al. Recommendations for the nomenclature of IgG4-related disease and its individual organ system manifestations. Arthritis Rheum. 2012; 64:3061–3067. [PubMed: 22736240]
4. Yamamoto M, Takahashi H, Ohara M, et al. A new conceptualization for Mikulicz's disease as an IgG4-related plasmacytic disease. Mod Rheumatol. 2006; 16:335–340. [PubMed: 17164992]
5. Geyer JT, Ferry JA, Harris NL, et al. Chronic sclerosing sialadenitis (Küttner tumor) is an IgG4-associated disease. Am J Surg Pathol. 2010; 34:202–210. [PubMed: 20061932]
6. Dahlgren M, Khosroshahi A, Nielsen GP, et al. Riedel's thyroiditis and multifocal fibrosclerosis are part of the IgG4-related systemic disease spectrum. Arthritis Care Res (Hoboken). 2010; 62:1312–1318. [PubMed: 20506114]
7. Kamisawa T, Okamoto A. Autoimmune pancreatitis: proposal of IgG4-related sclerosing disease. J Gastroenterol. 2006; 41:613–625. [PubMed: 16932997]
8. Khosroshahi A, Carruthers MN, Stone JH, et al. Rethinking Ormond's disease: 'idiopathic' retroperitoneal fibrosis in the era of IgG4-related disease. Medicine (Baltimore). 2013; 92:82–91. [PubMed: 23429355]
9. Della Torre E, Bozzolo EP, Passerini G, et al. IgG4-related pachymeningitis: evidence of intrathecal IgG4 on cerebrospinal fluid analysis. Ann Intern Med. 2012; 156:401–403. [PubMed: 22393144]
10. Mahajan VS, Mattoo H, Deshpande V, et al. IgG4-related disease. Annu Rev Pathol. 2014; 9:315–347. [PubMed: 24111912]
11. Khosroshahi A, Carruthers MN, Deshpande V, et al. Rituximab for the treatment of IgG4-related disease: lessons from 10 consecutive patients. Medicine (Baltimore). 2012; 91:57–66. [PubMed: 22210556]
12. Khosroshahi A, Bloch DB, Deshpande V, et al. Rituximab therapy leads to rapid decline of serum IgG4 levels and prompt clinical improvement in IgG4-related systemic disease. Arthritis Rheum. 2010; 62:1755–1762. [PubMed: 20191576]
13. Wallace ZS, Mattoo H, Carruthers M, et al. Plasmablasts as a biomarker for IgG4-related disease, independent of serum IgG4 concentrations. Ann Rheum Dis. 2015; 74:190–195. [PubMed: 24817416]
14. Mattoo H, Mahajan VS, Della-Torre E, et al. De novo oligoclonal expansions of circulating plasmablasts in active and relapsing IgG4-related disease. J Allergy Clin Immunol. 2014
15. Khosroshahi A, Stone JH. Treatment approaches to IgG4-related systemic disease. Curr Opin Rheumatol. 2011; 23:67–71. [PubMed: 21124087]
16. Parkes J, Roderick P, Harris S, et al. Enhanced liver fibrosis test can predict clinical outcomes in patients with chronic liver disease. Gut. 2010; 59:1245–1251. [PubMed: 20675693]
17. Abignano G, Cuomo G, Buch MH, et al. The enhanced liver fibrosis test: a clinical grade, validated serum test, biomarker of overall fibrosis in systemic sclerosis. Ann Rheum Dis. 2014; 73:420–427. [PubMed: 23511226]
18. Carruthers MN, Stone JH, Deshpande V, et al. Development of an IgG4-RD responder index. Int J Rheumatol. 2012; 2012:259408. [PubMed: 22611406]

19. Lichtinghagen R, Pietsch D, Bantel H, et al. The Enhanced Liver Fibrosis (ELF) score: normal values, influence factors and proposed cut-off values. J Hepatol. 2013; 59:236–242. [PubMed: 23523583]
20. Parkes J, Guha IN, Roderick P, et al. Enhanced Liver Fibrosis (ELF) test accurately identifies liver fibrosis in patients with chronic hepatitis C. J Viral Hepat. 2011; 18:23–31. [PubMed: 20196799]
21. Jordan S, Distler JH, Maurer B, et al. Effects and safety of rituximab in systemic sclerosis: an analysis from the European Scleroderma Trial and Research (EUSTAR) group. Ann Rheum Dis. 2015; 74:1188–1194. [PubMed: 24442885]
22. Keir GJ, Maher TM, Ming D, et al. Rituximab in severe, treatment-refractory interstitial lung disease. Respirology. 2014; 19:353–359. [PubMed: 24286447]
23. Geri G, Terrier B, Imbert-Bismut F, et al. Evolution of biomarkers of liver fibrosis and liver insufficiency in hepatitis C virus-infected patients treated with pegylated interferon plus ribavirin and rituximab. J Viral Hepat. 2012; 19:497–500. [PubMed: 22676362]
24. François A, Chatelus E, Wachsmann D, et al. B lymphocytes and B-cell activating factor promote collagen and profibrotic markers expression by dermal fibroblasts in systemic sclerosis. Arthritis Res Ther. 2013; 15:R168. [PubMed: 24289101]
25. Lighaam LC, Aalberse RC, Rispens T. IgG4-Related fibrotic diseases from an immunological perspective: regulators out of control? Int J Rheumatol. 2012; 2012:789164. [PubMed: 22701488]
26. Yang M, Rui K, Wang S, et al. Regulatory B cells in autoimmune diseases. Cell Mol Immunol. 2013; 10:122–132. [PubMed: 23292280]
27. Sato S, Hayakawa I, Hasegawa M, et al. Function blocking autoantibodies against matrix metalloproteinase-1 in patients with systemic sclerosis. J Invest Dermatol. 2003; 120:542–547. [PubMed: 12648215]
28. Pierson ER, Stromnes IM, Goverman JM. B cells promote induction of experimental autoimmune encephalomyelitis by facilitating reactivation of T cells in the central nervous system. J Immunol. 2014; 192:929–939. [PubMed: 24367024]
29. Wynn TA, Ramalingam TR. Mechanisms of fibrosis: therapeutic translation for fibrotic disease. Nat Med. 2012; 18:1028–1040. [PubMed: 22772564]
30. Wick G, Grundtman C, Mayerl C, et al. The immunology of fibrosis. Annu Rev Immunol. 2013; 31:107–135. [PubMed: 23516981]
31. Wynn TA. Cellular and molecular mechanisms of fibrosis. J Pathol. 2008; 214:199–210. [PubMed: 18161745]
32. Hinz B, Celetta G, Tomasek JJ, et al. α-smooth muscle actin expression upregulates fibroblast contractile activity. Mol Biol Cell. 2001; 12:2730–2741. [PubMed: 11553712]
33. Jiang F, Parsons CJ, Stefanovic B. Gene-expression profile of quiescent and activated rat hepatic stellate cells implicates Wnt signaling pathway in activation. J Hepatol. 2006; 45:401–409. [PubMed: 16780995]
34. Kisseleva T, Cong M, Paik Y, et al. Myofibroblasts revert to an inactive phenotype during regression of liver fibrosis. Proc Natl Acad Sci U S A. 2012; 109:9448–9453. [PubMed: 22566629]
35. Pratt WB. The mechanism of glucocorticoid effects in fibroblasts. J Invest Dermatol. 1978; 71:24–35. [PubMed: 355565]

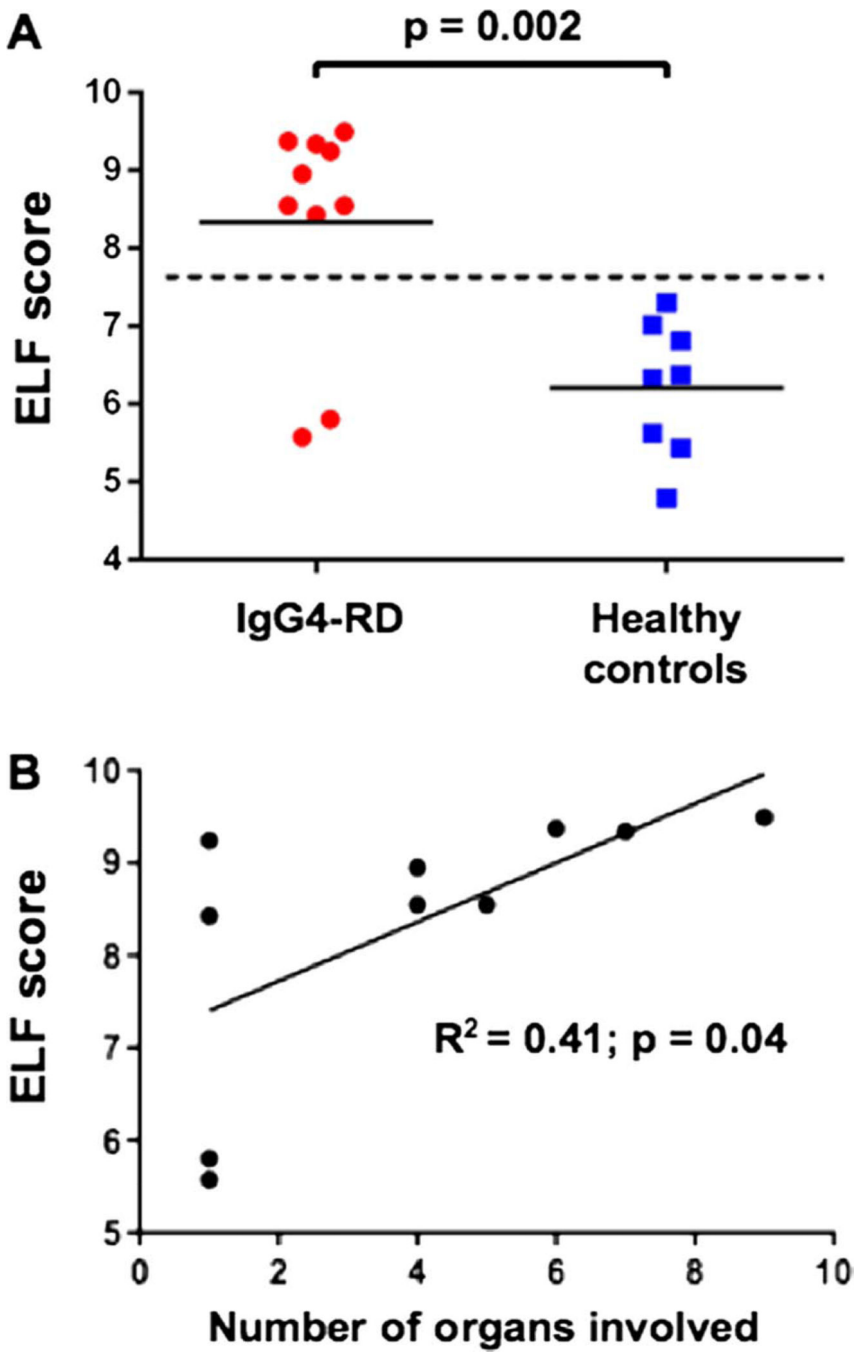

Figure 1.

Enhanced liver fibrosis (ELF) score is increased in IgG4-related disease (IgG4-RD) and correlates with the number of organs involved. (A) The ELF score is significantly increased in patients with IgG4-RD, compared with controls (p=0.002). (B) The ELF score correlates positively with the numbers of organs involved by IgG4-RD (R^2=0.41; p=0.04).

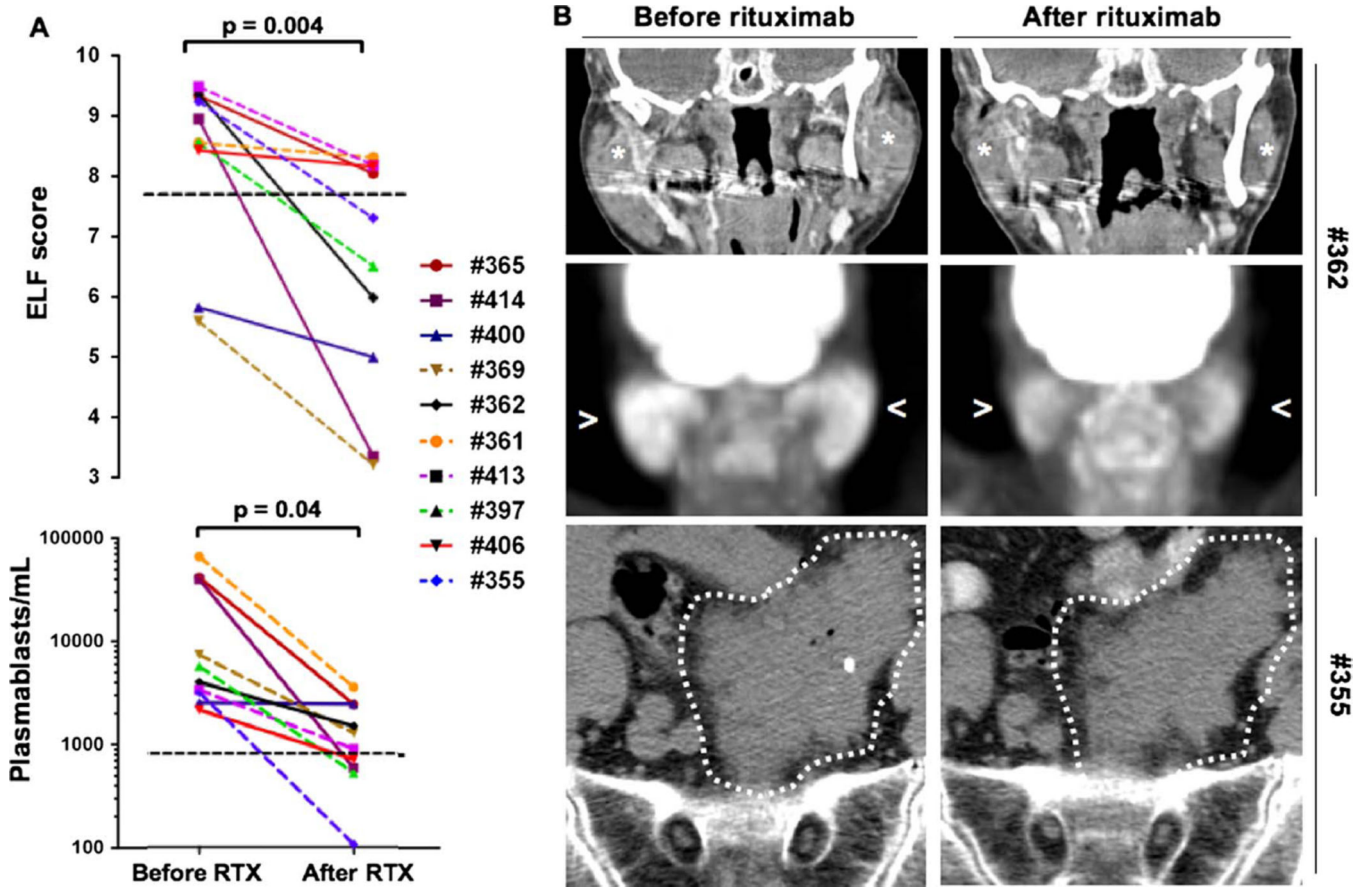

Figure 2.

Rituximab improves the overall degree of systemic fibrosis in IgG4-related disease. (A) Treatment with rituximab induces a significant reduction in the enhanced liver fibrosis (ELF) score and total circulating plasmablasts (paired t test analyses: p=0.004 and p=0.04, respectively). (B) CT scan (stars) and positron emission tomography scan (arrowheads) of the head and neck of Patient #362 showing a decrease in dimension and 18-fluorodeoxyglucose uptake of the parotid glands after rituximab. Abdominal CT scan of Patient #355 showing persistence of the retroperitoneal fibrotic mass after rituximab.

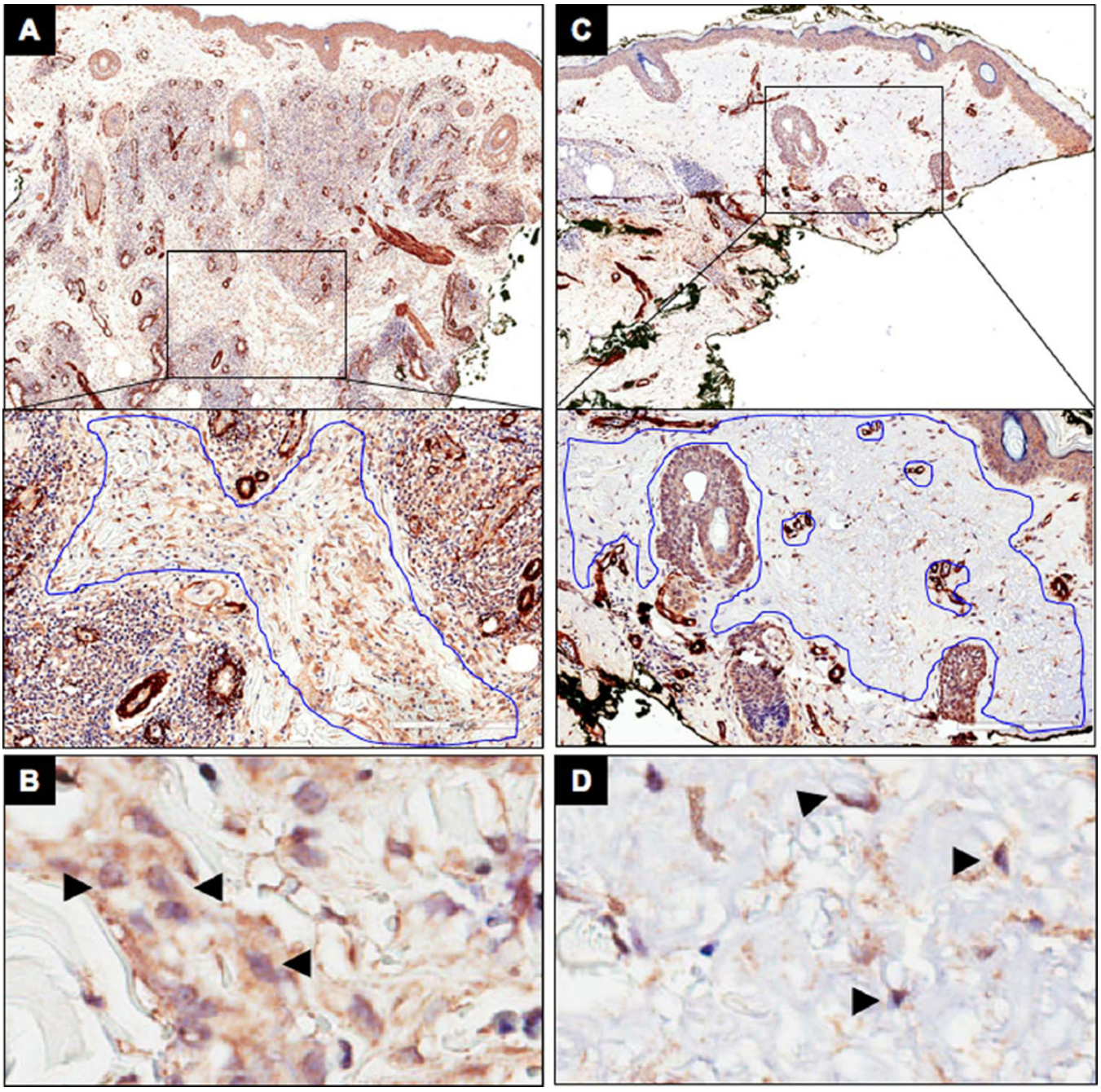

Figure 3.

Rituximab decreases dermal myofibroblast activation in IgG4-related disease (IgG4-RD) affected tissue. Immunohistochemistry for α-smooth muscle actin stain on skin biopsies from a patient with cutaneous IgG4-RD involvement, before (A and B) and after (C and D) treatment with rituximab. The number of moderately to strongly positive brown pixels per square micrometer decreases after rituximab in the regions containing predominantly dermal fibroblasts (outlined in blue) (original magnification: A and C 10×, inserts 20×). The morphology of individual fibroblasts before and after treatment is depicted at a higher magnification (40×) in B and D.

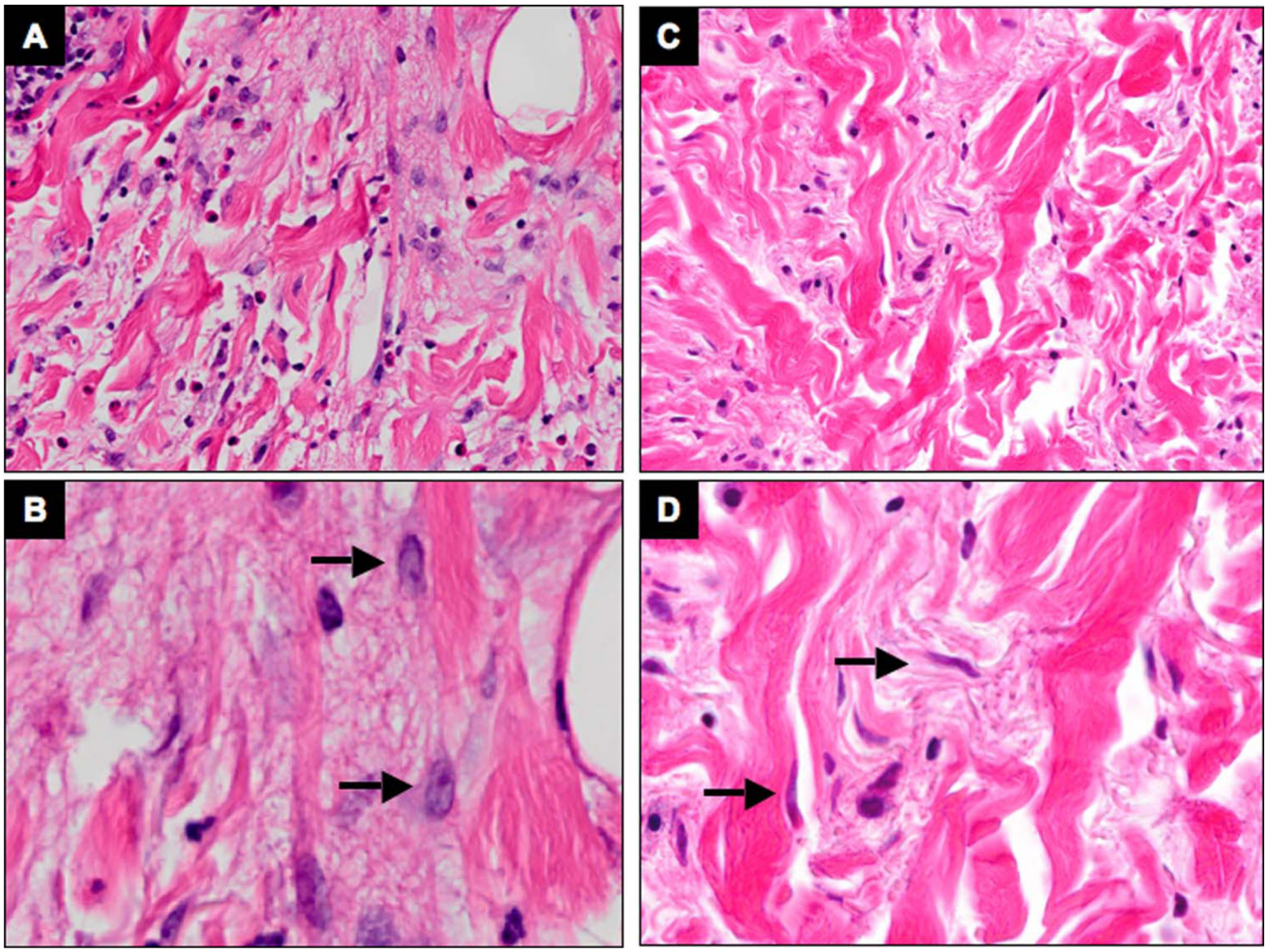

Figure 4.

Rituximab reduces myofibroblast volume in IgG4-related disease (IgG4-RD) lesions. H&E stain of consecutive skin biopsies from a patient with cutaneous IgG4-RD involvement from the same site, before (A and B) and after (C and D) treatment with rituximab. The dermal fibroblasts (arrows) exhibit abundant cytoplasm and large nuclei in active disease, and shrink after rituximab-mediated remission (original magnification: A and C 20×, B and D 40×).

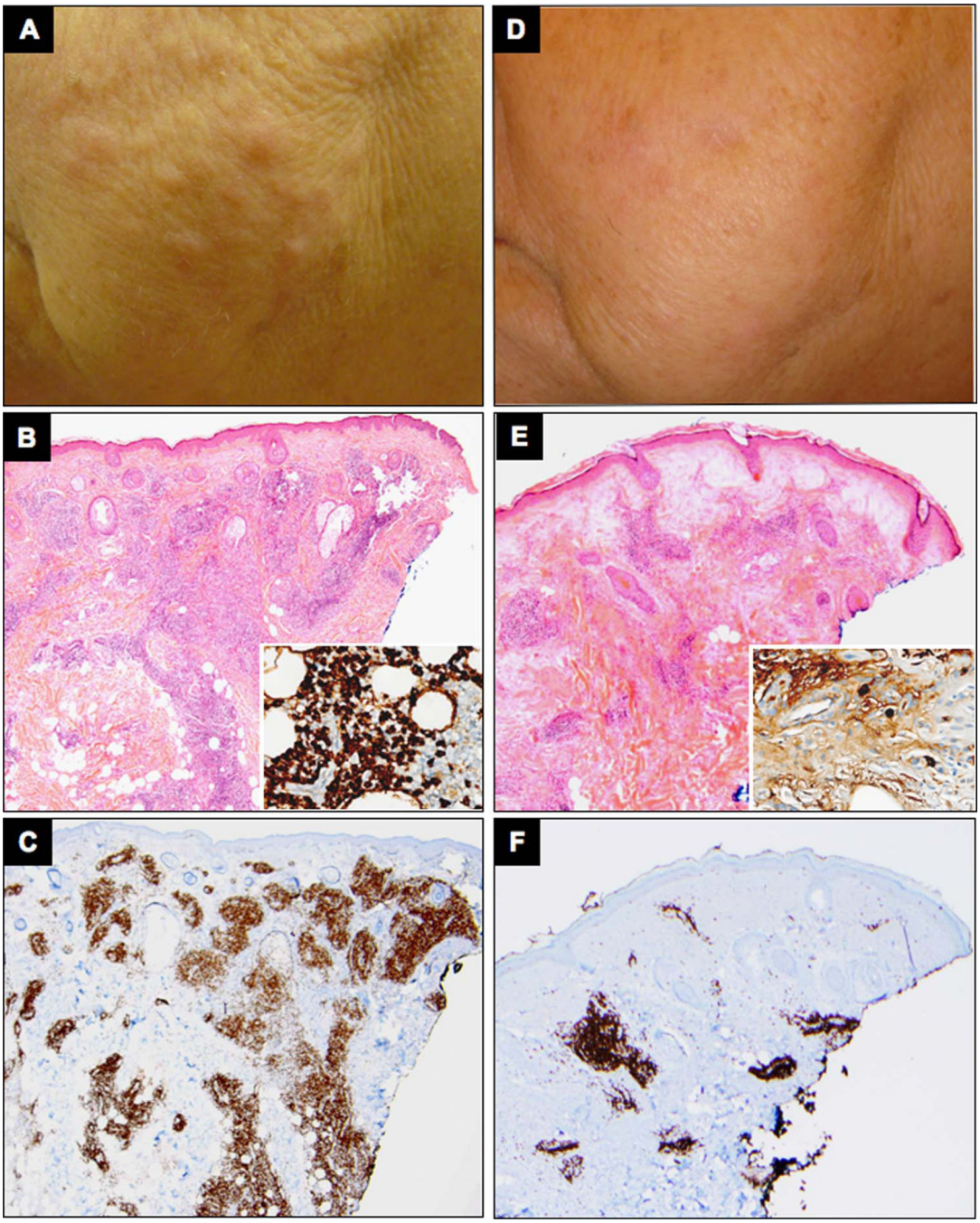

Figure 5.

Clinical response corresponds to decreased B and T lymphoplasmacytic infiltrate in IgG4-related disease (IgG4-RD) affected tissue. Clinical pictures from a patient with cutaneous IgG4-RD involvement before (A) and after (D) rituximab. H&E, and CD3 stain of skin biopsies before (B and C, respectively) and after (E and F, respectively) treatment with rituximab (original magnification 10×). Immunohistochemistry for IgG4 before (B) and after (E) rituximab is shown in inserts (original magnification 20×).

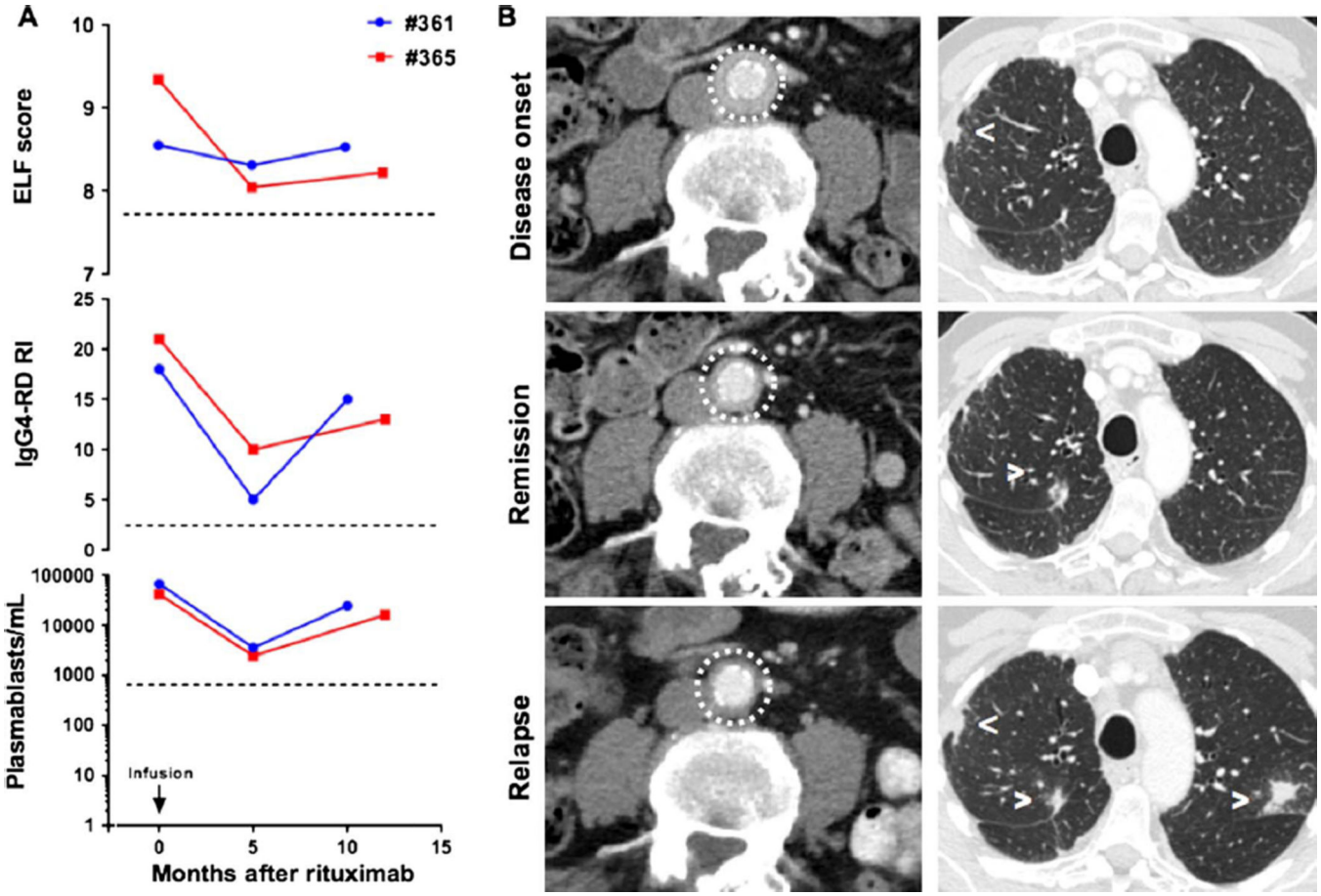

Figure 6.

IgG4-related disease (IgG4-RD) relapse corresponds to a new increase in the enhanced liver fibrosis (ELF) score. (A) Time course of ELF scores, IgG4-Responder Index and circulating plasmablasts after rituximab therapy in two patients who relapsed (#361 and #365) after initial treatment. (B) CT scan of Patient 365 showing the course of IgG4-RD lesions in the lung (arrowheads) and retroperitoneum (circle) at disease onset, remission and relapse.